ISBN: 978-3-95450-262-2 ISSN: 2673-5350 doi: 10.18429/JACoW-IBIC2025-WEPMO07

GAIN CALIBRATION FOR ELIMINATING X-Y COUPLING IN X-RAY BEAM POSITION MONITORS AT SPring-8 PHOTON BEAMLINES

Hideki Aoyagi†
Japan Synchrotron Radiation Research Institute (JASRI/SPring-8), Hyogo, Japan

Abstract

Although synchrotron radiation originates from charged particle beams, monitoring its positional stability requires distinct technical approaches. To enhance the accuracy of position and angle measurements of the synchrotron radiation beam at SPring-8 BL15XU, both a quadrant-type XBPM and a fixed-blade XBPM were installed on the same beamline. In the quadrant-type XBPM, widening the detector spacing led to noticeable X-Y coupling. To address this, a 2×2 correction matrix was introduced to perform linear transformation of the measured signals. The proposed method successfully eliminated X-Y coupling while maintaining resolution, enabling simultaneous operation of both XBPMs.

INTRODUCTION

At the synchrotron radiation facility SPring-8, X-ray Beam Position Monitors (XBPMs) based on photoelectron emission are installed at the front end of each beamline to measure angular fluctuations of the synchrotron radiation beam emitted from the light source [1]. The horizontal and vertical position sensitivity coefficients (correction factors) are determined by shifting the monitor body from its reference position in each direction and analyzing the output signals from four detectors.

However, synchrotron radiation beam generated by the fringe field of the bending magnet can generally induce slight horizontal–vertical coupling (hereafter referred to as X-Y coupling). This effect tends to become more pronounced as the distance to the tip of blade-shaped detectors increases.

To enhance the accuracy of both position and angle measurements, a second XBPM was added. Therefore, at BL15XU, a quadrant-type XBPM with independently adjustable detector spacing was installed approximately 20 m upstream from the source, while a conventional fixed-blade XBPM was installed approximately 25 m downstream. This configuration was designed to prevent the upstream XBPM's detectors from obstructing the synchrotron beam. However, increasing the detector spacing in the quadrant-type XBPM resulted in noticeable X-Y coupling in the correction factors, limitating on simultaneous operation of both XBPMs.

Several methods have been reported for correcting relative gain deviations between electrodes in electron beam position monitors of storage rings, such as beam-based gain calibration [2–4] and fast determination of BPM offsets from quadrupole magnet centers [5]. We propose a simple calibration method that effectively eliminates X-Y coupling in the correction factors. This method introduces

† aoyagi@spring8.or.jp

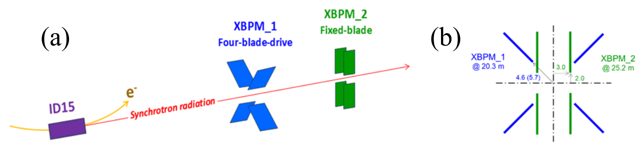

Figure 1: (a) XBPM_1 is positioned to avoid interference with XBPM_2. (b) Blade tips of XBPM_1 are set 4.6 mm from the center, corresponding to a projected distance of 5.7 mm at the XBPM_2 location.

a new formula to calculate the components of a 2×2 transformation matrix using only four measurement points—up, down, left, and right—enabling accurate mapping through linear transformation.

This report presents a quantitative evaluation of X-Y coupling in the quadrant-type XBPM, the procedure of the proposed calibration method, and experimental results obtained by intentionally modifying the electron beam orbit to verify the XBPM response characteristics.

X-Y COUPLING IN XBPM

This section presents a quantitative evaluation of X-Y coupling and discusses relevant design constraints. At BL15XU, a quadrant-type XBPM and a fixed-blade XBPM were installed at the upstream (20.3 m from the light source) and downstream (25.2 m), respectively, of the photon beamline frontend (Fig. 1(a)). The upstream XBPM_1 features independently adjustable blade detectors, allowing it to avoid interference with the downstream XBPM_2. The XBPM_2 is the standard model used in SPring-8 insertion device beamlines, with blade tips are fixed at ±3.0 mm horizontally and ±2.0 mm vertically from the center. To prevent obstruction, the blade tips of the XBPM_1 must be positioned at least 3.8 mm from the center. In practice, a safety margin was added, resulting in a tip position of 4.6 mm (Fig. 1 (b)).

To evaluate the degree of X-Y coupling in the output of the quadrant-type XBPM (calculated as the difference-over-sum of the four signals), the blade tip positions were varied to scan across the X-Y plane. The resulting plots of the difference-over-sum values are shown in Fig. 2. Ideally, the measured points should align with the vertices of a square lattice. However, the actual measurements revealed distortions, indicating that even when the beam is displaced purely in the horizontal or vertical direction, the XBPM output erroneously includes components from the orthogonal axis. This distortion—i.e., the increase in X-Y coupling—was found to intensify as the blade tips moved farther from the center.

To mitigate X-Y coupling, it is necessary to optimize the blade tip positions while maintaining sufficient detector current for resolution. Furthermore, applying a new correc-

ISBN: 978-3-95450-262-2 ISSN: 2673-5350 doi: 10.18429/JACoW-IBIC2025-WEPMO07

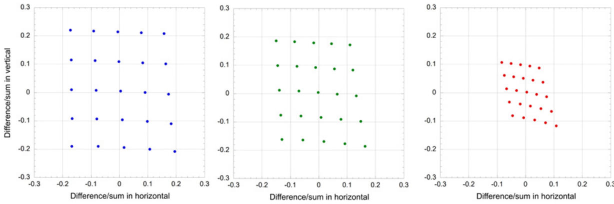

(a) 2.8 mm (b) 3.4 mm (c) 4.6 mm

Figure 2: Difference-over-sum scan results for XBPM_1 at various blade tip positions: (a) 2.8 mm, (b) 3.4 mm, and (c) 4.6 mm from the center. Increased tip distance leads to reduced sensitivity and enhanced X-Y coupling.

tion matrix that effectively eliminates X-Y coupling is essential for accurate measurements.

CORRECTION MATRIX

To address the distortion observed in Fig. 2, a correction matrix was introduced to linearly transform the measured difference-over-sum values and eliminate X-Y coupling. This matrix takes the form of a 2×2 transformation matrix applied to the XBPM output. To determine its four components, a beam-based calibration was performed by mechanically shifting the XBPM body and observing the XBPM response, rather than displacing the synchrotron radiation beam. Four points (±Δx and ±Δy around the origin) were selected to be consistent with the traditional method of calculating correction factors.

As illustrated by the green dots in Fig. 3, the coordinates of the four observed XBPM output points (labeled **a** to **d**) are defined as follows,

a: (x_a, y_a), **b**: (x_b, y_b), **c**: (x_c, y_c), **d**: (x_d, y_d) .

The horizontal and vertical difference-over-sum values (x, y) are calculated using the following equations:

$$\text{Horizontal:}\ x = \frac{(UR+LR)-(UL+LL)}{UL+UR+LL+LR},$$

$$\text{Vertical:}\ y = \frac{(UL+UR)-(LL+LR)}{UL+UR+LL+LR},$$

here, UL, UR, LL, and LR represent the output signals from the upper-left, upper-right, lower-left, and lower-right detectors, respectively.

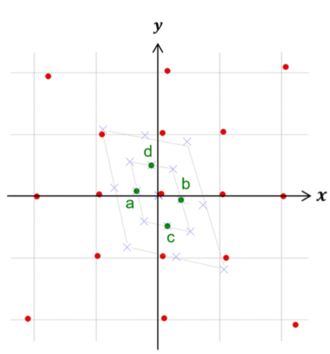

Figure 3: Mapping of XBPM output for coupling compensation. Green dots represent the four calibration points. Distorted measurements (blue ×) are transformed into square lattice vertices (red ●) using the correction matrix.

Table 1: Correction Matrices

Matrix Type	XBPM_1 (quadrant-type)	XBPM_2 (fixed-blade)
Initial Matrix ***A***	$\begin{pmatrix} 2.96 & 0.77 \\ 0.44 & 2.15 \end{pmatrix}$	$\begin{pmatrix} 0.21 & -0.01 \\ 0.00 & 0.76 \end{pmatrix}$
Intermediate Matrix ***A'***	$\begin{pmatrix} 0.94 & -0.06 \\ -0.03 & 1.12 \end{pmatrix}$	$\begin{pmatrix} 5.79 & -0.25 \\ -0.41 & 1.83 \end{pmatrix}$
Refined Matrix ***A''*** (= $\boldsymbol{A'} \cdot \boldsymbol{A}$)	$\begin{pmatrix} 2.81 & 0.86 \\ 0.57 & 2.60 \end{pmatrix}$	$\begin{pmatrix} 1.23 & -0.12 \\ -0.09 & 1.38 \end{pmatrix}$

Conventional Correction Coefficients

The conventional correction coefficients can be calculated using the following equations:

$$Ax = \frac{2\,\Delta x}{(x_b - x_a)}, \qquad Ay = \frac{2\,\Delta y}{(y_d - y_c)}.$$

These coefficients form a diagonal 2×2 matrix:

$$\begin{pmatrix} x' \\ y' \end{pmatrix} = \begin{pmatrix} Ax & 0 \\ 0 & Ay \end{pmatrix} \begin{pmatrix} x \\ y \end{pmatrix}.$$

This approach assumes no cross-axis interference, which is insufficient when X-Y coupling is present.

Correction Matrix for Eliminating X-Y Coupling

To eliminate X-Y coupling, a refined correction matrix A was derived by analyzing the same four measurement points employed in the previous section. The matrix is expressed as:

$$\begin{pmatrix} x'' \\ y'' \end{pmatrix} = \boldsymbol{A} \begin{pmatrix} x \\ y \end{pmatrix} = \frac{\mathbf{1}}{\mathbf{1} - \boldsymbol{\alpha\beta}} \begin{pmatrix} \mathbf{1} & \boldsymbol{\alpha} \\ \boldsymbol{\beta} & \mathbf{1} \end{pmatrix} \begin{pmatrix} Ax & 0 \\ 0 & Ay \end{pmatrix} \begin{pmatrix} x \\ y \end{pmatrix}.$$

The coupling parameters α and β are defined as:

$$\boldsymbol{\alpha} = -Ax \times \frac{(x_d - x_c)}{2\Delta x}, \qquad \boldsymbol{\beta} = -Ay \times \frac{(y_b - y_a)}{2\Delta y}.$$

The resulting correction matrix ***A***, calculated using this method, is presented in the first row of Table 1, which summarizes the transformation coefficients.

Verification of the 2×2 Correction Matrix A

To verify the effectiveness of matrix ***A***, a wide-area scan across the X-Y plane was performed using XBPM_1. As shown in Fig. 4, the corrected XBPM output values (red circles) align with the vertices of a square lattice, indicating

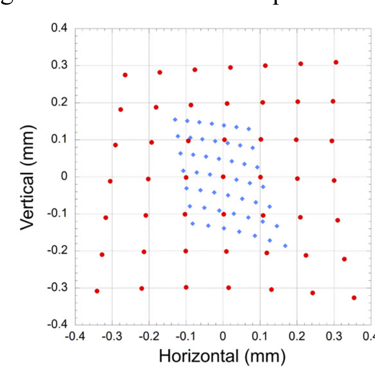

Figure 4: Scan measurement of XBPM_1 using correction matrix ***A*** (red ●). The blue "♦" represent values before transformation.

ISBN: 978-3-95450-262-2 ISSN: 2673-5350 doi: 10.18429/JACoW-IBIC2025-WEPMO07

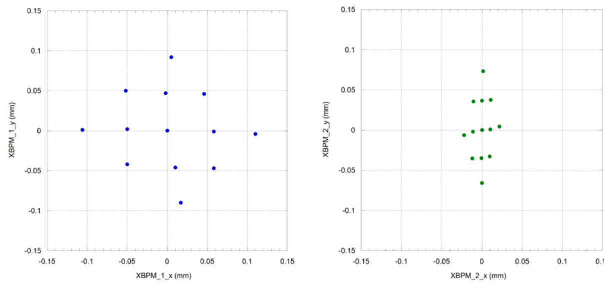

(a) XBPM_1 (b) XBPM_2

Figure 5: XBPM responses to angular beam displacement using correction matrix A. XBPM_1 shows consistent behavior, while XBPM_2 exhibits reduced sensitivity and X-Y coupling due to beam profile constraints.

successful compensation of X-Y coupling. In contrast, the uncorrected values (blue diamonds) exhibit noticeable distortion.

Although slight curvature remains in some red points due to the linear nature of the transformation, the residual distortion is within a practically acceptable range. The method enables accurate correction without extra measurements.

EVALUATION OF XBPM RESPONSE

To evaluate the ability of XBPMs to detect angular deviations of the synchrotron radiation beam, a localized bump was applied to the electron beam orbit, inducing controlled angular shifts. The resulting beam displacements were measured using both XBPM_1 and XBPM_2. The measurement points were configured with angular steps of ±2.5 μrad in both horizontal and vertical directions.

Response of XBPMs Using Correction Matrix

Figure 5 presents the output responses of XBPM_1 and XBPM_2 when the beam angle was varied using the localized bump. XBPM_1 exhibited a response pattern largely consistent with theoretical expectations, although a slight underestimation was observed in the vertical component. In contrast, XBPM_2 showed reduced sensitivity, particularly in the horizontal direction, and exhibited noticeable X-Y coupling. This behavior is attributed to the aperture of the main mask located between XBPM_1 and XBPM_2, which constrains the synchrotron radiation profile and affects downstream measurements.

Refinement of the Correction Matrix

To compensate for the reduced response of XBPM_2, the correction matrix was refined. A new set of measurements was taken at four angular displacement points of ±5 μrad in the up, down, left, and right directions. Based on these measurements, an intermediate correction matrix ***A'*** was derived. The final refined matrix ***A''*** was then obtained by left-multiplying the original matrix ***A*** with ***A'***, i.e., ***A''=A'· A***. Both matrices are summarized in Table 1. In Fig. 6 (a), the output of XBPM_1 forms a square grid, confirming that X-Y coupling has been effectively eliminated.

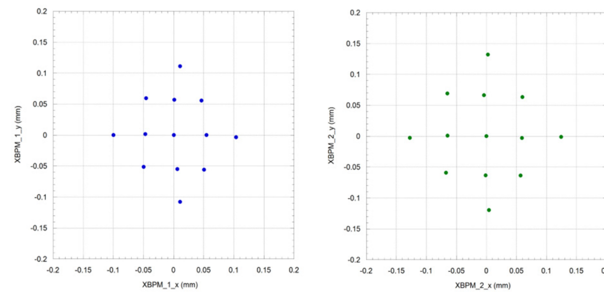

(a) XBPM_1 (b) XBPM_2

Figure 6: XBPM responses using refined correction matrix ***A''***. (a) XBPM_1 output forms a square grid, indicating successful elimination of X-Y coupling. (b) XBPM_2 output shows improved symmetry and reduced coupling, compensating for profile restrictions.

In Fig. 6 (b), the output of XBPM_2 shows improved symmetry and reduced coupling, indicating successful compensation for the effects of the beam profile restriction.

CONCLUSION

To improve the accuracy of synchrotron radiation beam monitoring at SPring-8 BL15XU, a quadrant-type XBPM was installed upstream, and a conventional fixed-blade XBPM downstream. However, increased blade spacing in the quadrant-type XBPM introduced X-Y coupling, limiting simultaneous operation.

To address this issue, a 2×2 correction matrix was developed using four beam-based calibration points. This matrix effectively eliminated X-Y coupling through linear transformation, restoring the output to a square lattice pattern without requiring additional measurements.

Experimental validation using localized beam bumps confirmed the improved response of the quadrant-type XBPM. Although the downstream XBPM exhibited reduced sensitivity due to beam profile constraints, refinement of the correction matrix compensated for this effect, enabling accurate angle detection.

These results demonstrate that the proposed calibration method enhances XBPM performance under constrained geometries. Future work will focus on automating the correction process and evaluating long-term stability.

ACKNOWLEDGMENTS

We would like to express our sincere gratitude to the accelerator operators at SPring-8 for their invaluable support in facilitating the smooth execution of the experiment. We are especially grateful to Mr. Koji Motomura and colleagues at Engineering Team of the RIKEN SPring-8 Center (RSC) for their prompt and insightful assistance in implementing the 2×2 correction matrix into the BL-774 beamline control and data acquisition system. We also thank Mr. Yasuhisa Matsuzaki of the Beamline Optics Division at the Japan Synchrotron Radiation Research Institute (JASRI) for cross-checking the formula for calculating the correction matrix, as well as the division staff for their technical support.

ISBN: 978-3-95450-262-2 ISSN: 2673-5350 doi: 10.18429/JACoW-IBIC2025-WEPMO07

REFERENCES

[1] H. Aoyagi, T. Kudo, and H. Kitamura, “Blade-type X-ray beam position monitors for SPring-8 undulator beamlines,” *Nucl. Instrum. Methods Phys. Res. A*, vol. 467–468, pp. 252–255, Jul. 2001. doi:10.1016/s0168-9002(01)00292-3

[2] M. Masaki *et al.*, “A Method of Beam-based Calibration for Beam Position Monitor”, in *Proc. 11th Symposium on Accelerator Science and Technology*, Kamigori, Hyogo, Japan, pp. 83-85, 1997.

[3] T. Fujita *et al.*, “Long-Term Stability of the Beam Position Monitors at SPring-8”, in *Proc. IBIC'15*, Melbourne, Australia, Sep. 2015, pp. 359-363. doi:10.18429/JACoW-IBIC2015-TUPB020

[4] M. Tejima *et al.*, “Beam Based Gain Calibration of Beam Position Monitors at J-PARC MR”, in *Proc. DIPAC’11*, Hamburg, Germany, May 2011, paper MOPD22, pp.92-94.

[5] H. Maesaka *et al.*, “Fast beam-based alignment of BPMs and quadrupole magnets for SPring-8-II”, presented at IBIC2025, Liverpool, UK, Sep. 2025, paper WEPCO07, this conference.